7342–7356 *Nucleic Acids Research, 2023, Vol. 51, No. 14* *Published online 16 June 2023*
https://doi.org/10.1093/nar/gkad515

The CSB chromatin remodeler regulates PARP1- and PARP2-mediated single-strand break repair at actively transcribed DNA regions

Rabeya Bilkis[1,2,3], Robert J. Lake[1,2], Karen L. Cooper[4], Alan Tomkinson[1,2] and Hua-Ying Fan[1,2,*]

[1]Program in Cell and Molecular Oncology, University of New Mexico Comprehensive Cancer Center, Albuquerque, NM 87131, USA, [2]Division of Molecular Medicine, Department of Internal Medicine, University of New Mexico Health Science Center, Albuquerque, NM 87131, USA, [3]Biomedical Sciences Graduate Program, University of New Mexico Health Science Center, Albuquerque, NM 87131, USA and [4]Department of Pharmaceutical Sciences, College of Pharmacy, University of New Mexico Health Sciences Center, Albuquerque, NM 87131, USA

Received December 31, 2022; Revised May 03, 2023; Editorial Decision May 27, 2023; Accepted June 01, 2023

ABSTRACT

Efficient repair of oxidized DNA is critical for genome-integrity maintenance. Cockayne syndrome protein B (CSB) is an ATP-dependent chromatin remodeler that collaborates with Poly(ADP-ribose) polymerase I (PARP1) in the repair of oxidative DNA lesions. How these proteins integrate during DNA repair remains largely unknown. Here, using chromatin co-fractionation studies, we demonstrate that PARP1 and PARP2 promote recruitment of CSB to oxidatively-damaged DNA. CSB, in turn, contributes to the recruitment of XRCC1, and histone PARylation factor 1 (HPF1), and promotes histone PARylation. Using alkaline comet assays to monitor DNA repair, we found that CSB regulates single-strand break repair (SSBR) mediated by PARP1 and PARP2. Strikingly, CSB's function in SSBR is largely bypassed when transcription is inhibited, suggesting CSB-mediated SSBR occurs primarily at actively transcribed DNA regions. While PARP1 repairs SSBs at sites regardless of the transcription status, we found that PARP2 predominantly functions in actively transcribed DNA regions. Therefore, our study raises the hypothesis that SSBR is executed by different mechanisms based on the transcription status.

GRAPHICAL ABSTRACT

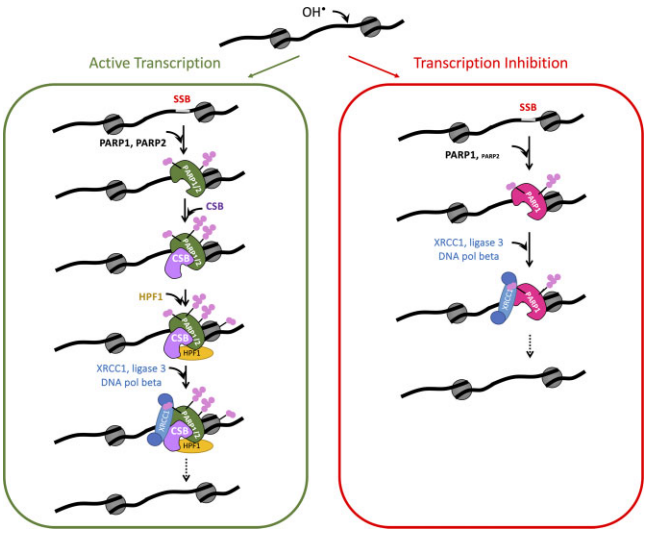

INTRODUCTION

Oxidative stress underlies numerous pathologies, including cancer, inflammation, and neurological disorders/neurodegeneration (1,2). Reactive oxygen species (ROS) are constantly generated during normal cellular metabolism. The hydroxyl radical is the major cause of ROS-induced DNA damage; it attacks both the sugar of the phosphodiester backbone and the DNA bases. These two types of DNA lesions are repaired by single-strand break repair (SSBR) and base-excision repair (BER), respectively (3–5). These pathways differ only in the initial recognition and processing of the DNA lesion, with subsequent steps being shared. SSBs are sensed by the Poly(ADP-ribose) polymerases 1 and 2 (PARP1/2),

*To whom correspondence should be addressed. Tel: +1 505 272 1085; Email: hufan@salud.unm.edu

enzymes that are activated by their binding to SSBs. Activated PARP1/2 covalently link chains of ADP-ribose molecules, derived from NAD^+, to themselves as well as additional proteins, an activity termed PARylation. PARP1 accounts for ∼80–90% of DNA damage-activated PARylation in human cells, with PARP2 contributing most of the remaining activity (6,7). Histone PARylation Factor 1 (HPF1) alters the substrate specificity of PARP1/2, from primarily aspartate and glutamate residues to serine residues. Serine PARylation is most relevant during the DNA-damage response, with the major substrates being the histone proteins (8–12). The scaffold protein XRCC1 is then recruited to SSB sites by binding to PARylated PARP1 or 2, bringing with it associated SSBR enzymes, such as PNKP, DNA ligase 3 and DNA polymerase β, to repair the breaks (3).

Cockayne syndrome (CS) is a premature aging syndrome. In addition, individuals with CS suffer from extreme sun sensitivity and have developmental and neurological abnormalities (13–15). Mutations in the gene encoding for the Cockayne syndrome group B (CSB) protein account for the majority of Cockayne syndrome cases. CSB is a member of the Swi2/Snf2 family of ATP-dependent chromatin remodelers (16) and interacts with PARP1; however, the functional consequences of this interaction are unknown (17). Swi2/Snf2 chromatin remodelers use the energy from ATP hydrolysis to alter DNA-histone contacts and regulate chromatin access for factor binding (18). Additionally, some remodelers can alter contacts between non-histone proteins and DNA, such as transcription factors (19,20). CSB activity is critical for the relief of genotoxic stress created by both UV irradiation and oxidizing agents (21–30). UV irradiation creates transcription-blocking, bulky DNA lesions that are repaired by a CSB-dependent pathway called transcription-coupled nucleotide excision repair (TC-NER) (24,31). In TC-NER, CSB is recruited to DNA lesion-stalled RNA polymerase II in a manner dependent upon ATP hydrolysis (22). Once bound to sites of DNA lesions, CSB initiates the recruitment of the nucleotide excision repair proteins (32). In addition, it has been suggested that CSB's ATP-dependent chromatin remodeling activity creates a chromatin environment conducive for repair and transcription resumption after repair (23). To date, there is no evidence indicating that PARP1 participates in TC-NER.

While CSB also regulates the repair of oxidative DNA lesions, a process that requires PARP1/2, the role of CSB in this repair process is largely unknown (26). It remains controversial as to whether ROS-induced DNA damage is repaired in a transcription-coupled manner. This may be explained in part because of the wide spectrum of ROS-induced DNA lesions that include base modifications and sugar damage. Interestingly, cells derived from Cockayne syndrome patients have elevated ROS levels, and CSB-deficient cells are hypersensitive to oxidative stress (27,33). Live cell imaging has revealed that CSB rapidly accumulates at sites of locally-induced oxidative DNA damage (34). Moreover, CSB contains a PAR-binding module (PBM) with demonstrated PAR-binding activity (35,36). Additionally, purified CSB has been shown to remove PARP1 from DNA, albeit with modest activity (36). We previously found PARP1-null mutations rescue the severe sensitivity of CSB deficiency to oxidative stress (37). Given that prolonged PARP1 retention on chromatin is thought to be more damaging than loss of PARP1 activity, as this can lead to NAD^+ depletion, these finding suggest the possibility that regulation of PARP1 activity is a critical CSB function during oxidative stress and, in the absence of PARP1, this CSB activity is no longer needed (37). In support of this hypothesis, we found that CSB recruitment to oxidized chromatin is regulated by the PARP1 protein and occurs independently of ATP hydrolysis by CSB (22,38). This CSB-recruitment mechanism contrasts with that used during TC-NER, which requires ATP hydrolysis by CSB and is PARP1 independent (22,38). Therefore, the CSB-chromatin targeting mechanisms used during TC-NER and oxidative DNA-damage repair are fundamentally different.

In this study, we monitored DNA-damage repair, cell viability, and the association of DNA repair proteins with chromatin during oxidative stress, to dissect the function of CSB in SSBR. Our analysis has uncovered a SSBR regulatory mechanism that is dedicated to the repair of oxidative DNA damage in actively transcribed DNA regions and requires the coordination of CSB and PARP1/2 activities.

MATERIALS AND METHODS

Alkaline comet assay

Approximately 8×10^4 cells were seeded on 60 mm dishes. The following day, cells were treated with 50 μM H_2O_2 in PBS (Ca^{2+} and Mg^{2+} free) for 15 min on ice. H_2O_2 was then removed and cells were rinsed once with PBS and allowed to repair in fresh medium for 30 min in a 37°C incubator with 5% CO_2. For all samples, including untreated or no-repair samples, cells were rinsed with PBS, trypsinized and resuspended in PBS at 1×10^5 cells/ml. Cells were then mixed with 1% low-gelling-temperature agarose (Sigma, cat. no. A4018, St. Louis, MO, USA) in PBS, warmed to 37°C, at a ratio of 1: 10 (v/v), and spotted on a 20-well CometSlide in duplicate (R&D systems, cat. no. 4252-500-01, Minneapolis, MN, USA). After gelling, slides were immersed in Lysis Buffer (2.5 M NaCl, 100 mM EDTA (pH 8.0), 10 mM Tris–HCl pH 10, 0.1% Triton X-100) for 30 min (CS1AN-derived cell lines) or 45 min (RPE1-derived cell lines) at 4°C. Slides were then incubated in Denaturing Solution (0.2 M NaOH, 1 mM EDTA, pH 8.0) for 30 min. Electrophoresis was performed at 21 V for 30 min in Denaturing Solution. After electrophoresis, slides were washed twice with water, once with 70% ethanol, and air-dried overnight (protected from light). The next day, DNA was stained with SYBR Gold (Invitrogen, cat. no. S11494, Carlsbad, CA, USA) solution diluted at 1:10 000 in 20 mM Tris–HCl, pH 7.4. Images were captured using an Olympus XI83 fluorescence microscope with a DP72 camera and cellSens Dimension Software (Olympus America; ver. 1.17, Tokyo, Japan). Comet Analysis Software (Trevigen, Inc. ver. 1.2, Gaithersburg, MD, USA) was used to analyze images. 100–150 cells were scored per experiment, unless otherwise stated. Images were manually reviewed to exclude overlapping cells as well as procedural artifacts. The level of DNA breaks was expressed as tail moment.

Cell culture and generation of clonal stable cell lines

CS1AN- and RPE-1-derived cell lines were cultured in DMEM/F12 medium supplemented with 10% FBS (6,15,22,39). 293T cells were cultured in DMEM supplemented with 10% FBS. Flag-tagged CSB^{WT} and CSB^{K538A} were expressed from the pBABE-PURO vector (Dr Alan Weiner, University of Washington). These constructs were transfected into CS1AN-sv cells with lipofectamine 2000 (Invitrogen) and selected with 250 ng/ml puromycin. Single colonies were picked to generate clonal cell lines. Western blot and immunofluorescence analyses were used to characterize the stable cell lines. Clonal cell lines with CSB levels similar to that of MRC5, a diploid fibroblast line, were selected for experiments (22). CS1AN-sv cells are referred as CSB^{null} cells. CS1AN-sv cells stably expressing the wildtype CSB protein are referred to as CSB^{WT} cells.

Cell treatment

Menadione (MP Biomedicals, cat. no. 102259, Solon, OH, USA) was dissolved in 100% ethanol to make 100 mM stock solution. 30% H_2O_2 (Avantor, cat. no. 2190-03, Radnor, PA, USA) was freshly diluted in 1× PBS to final concentrations of 150 μM or 50 μM, and then directly added to cells. α-amanitin (Cayman Chemical Co., cat. no. 17898, Ann Arbor, MI, USA) was dissolved in water to make a stock solution of 1 mg/ml and used at 1 μg/ml. 5,6-Dichlorobenzimidazole 1-β-D-ribofuranoside (DRB) (Sigma-Aldrich, cat. no. D1916) was used at 50 μM (38). The PARP inhibitor KU-0058948 hydrochloride (Axon Medchem, cat. no. 2001) and EB-47(dihydrochloride) (MedChem Express, HY-108631) were dissolved in DMSO to make a stock solution of 10 mM and used at a final concentration of 1 μM and 10 μM, respectively. α-amanitin, DRB, KU-0058948 or EB47 was added to cells 1 h before H_2O_2 (or menadione) treatment, during treatment and during the 30 min recovery.

shRNA-mediated knockdown

Predesigned lentiviral shRNA expression constructs were purchased from Sigma-Aldrich (St. Louis, MO, USA): CSB (TRCN0000016775, CGACAAATCTTCAAGCAGTTT), HPF1 (TRCN0000136219 and TRCN0000137670), and the non-mammalian shRNA control (SHC002). Lentivirus was produced using the third generation packaging plasmids as described previously (23). Target cells were plated to ∼20% confluence at the time of infection. Fresh medium was added 24h after infection. Cells were processed for analysis 72 h (for CSB) or 96 h (for HPF1) post-infection. The phenotypes associated with CSB KD in RPE-1 cells are unlikely due to an off-target effect (Figure 3), because the CSB^{null} cells displayed similar phenotypes in the alkaline comet and cell viability assays, as compared to the CSB^{WT} cells (Figure 1).

Co-immunoprecipitation experiments

The human PARP1 cDNA (GenBank: NC_000001.11) was purchased from Horizon Mammalian Gene Collection. The PARP2 cDNA is from John M. Pascal (40). HPF1 cDNA was obtained from AddGene, a gift from Thomas Muir (Addgene plasmid # 111577; http://n2t.net/addgene:111577; RRID:Addgene_111577) (41). The PARP1, PARP2 and HPF1 cDNA was PCR amplified and cloned into a Flag-pcDNA3 expression vector using gateway cloning technology (ThermoFisher Scientific).

HEK 293T were transfected with mammalian expression constructs (pHF72-23, HA-tagged CSB in pSVL, and Flag-tagged PARP1, Flag-tagged PARP2, or Flag-tagged HPF1 in pcDNA3) using PEI. Forty-eight hours post transfection, cells were treated with α-amanitin (1 μg/ml), and/or menadione (100 μM) as described above, washed with PBS, and collected in PBS containing 0.5% Triton X -100 on ice. Cell lysates were sonicated at 30% amplitude for 1 min using a Branson sonifier. Sonicated lysates were centrifuged at ∼21 000 × g for 10 min at 4°C, to remove insoluble material, followed by a 30 min incubation on ice before a final centrifugation at ∼21 000 × g for 30 min at 4°C. The supernatant was incubated with BSA-blocked anti-Flag M2 agarose beads (Sigma, cat. no. A2220, St. Louis, MO, USA) overnight at 4°C. Beads were subsequently washed three times with PBS containing 0.5% Triton-X-100 and then collected in 1 × SDS sample buffer.

Survival assays

Cell viability was determined by trypan blue exclusion. 2×10^5 cells were seeded in a 60 mm dish. The following day, cells were treated with H_2O_2 in PBS for 15 min at room temperature, or menadione for 1 h in growth medium at 37°C. Cells were then rinsed once with PBS and fresh medium was added. Cells were placed back in the incubator. After 24 h, cells were stained with trypan blue and the number of clear, viable cells were counted using a hemocytometer.

Protein fractionation, quantification and western blotting

For chromatin-enriched protein fractions, cells in a 60 mm dishes were rinsed once with 1× PBS and collected by scrapping in 200 μl buffer B on ice (22). Cell lysates were centrifugated at 21 000 × g for 15 min at 4°C. 200 μl 1× SDS sample buffer with no DTT or bromophenol blue was added to the cell pellet. Pellets were then sonicated with a Branson sonifier at 25% amplitude for 1 min. Soluble protein extracts were obtained by adding 50 μl of 1× SDS sample buffer to 150 μl of the supernatant obtained after centrifugation. Whole cell extracts were prepared by adding 200 μl of 1× SDS sample buffer without DTT and bromophenol blue directly to the plate of cells, and lysates were sonicated as described above. Protein concentration was determined using the Pierce BCA Protein Assay (Thermo Fisher, Waltham, MA, USA). After quantification, DTT and bromophenol blue were added to the samples, and ∼25 μg of total protein was resolved in a 4–12% Bis–Tris SurePAGE gel (GenScript, cat. no. M00653, NJ, USA) or a 4–12% Bis–Tris NuPAGE gel (ThermoFisiher, NP0323BOX) using MOPS-SDS buffer. Color Prestained Protein Standard was purchased from NEB (P7719S, Ipswich, MA, USA). Immunoblots were developed using either SuperSignal West Pico (ThermoFisher) or Western-Bright Quantum (Advansta, cat. no. K-12042-D10, San

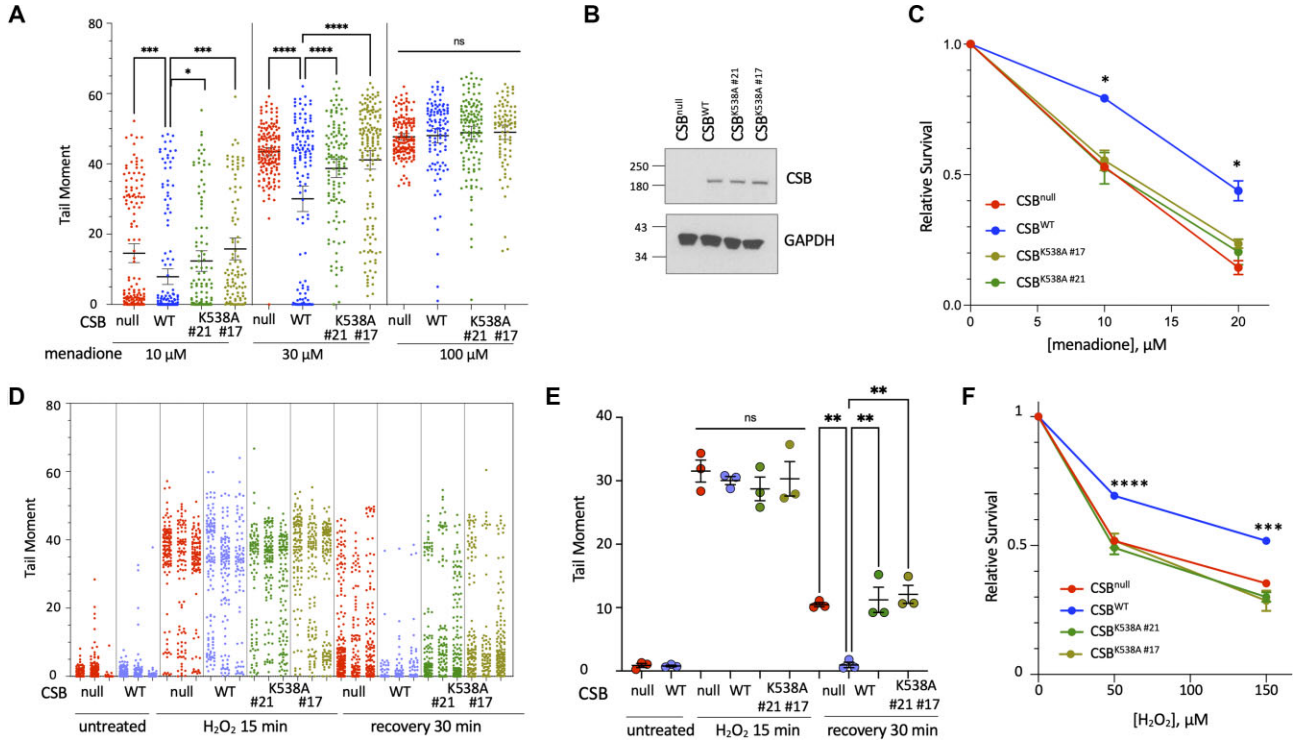

Figure 1. CSB regulates oxidative DNA-damage repair in an ATP-dependent manner. (**A**) Alkaline comet assays measuring SSBs in CSB^{null} cells, CSB^{null} cells reconstituted with wildtype CSB (WT) and two clonal cell lines expressing an ATPase-deficient CSB derivative (K538A), after a 1-hour menadione treatment at the indicated concentrations. Relative levels of DNA lesions are expressed as 'tail moment' (43). Each dot represents the tail moment of a single cell, with 100–150 cells counted per condition. Horizontal bars represent the means ± 95% CI. Statistical significance was determined using one-way ANOVA with Holm-Sidak's multiple comparison test using a single pooled variance; *$P \leq 0.05$, ***$P \leq 0.001$, ****$P \leq 0.0001$, ns: $P > 0.05$. (**B**) Western blot analysis of cell lines used in the comet assays showing relative CSB expression levels. (**C**) Menadione survival assays. Two clonal cell lines expressing an ATPase defective CSB derivative were compared to the CSB^{WT} and CSB^{null} cell lines. Shown are means ± SEM of two independent experiments. An unpaired *t*-test was used to calculate the statistical significance. *$P < 0.05$, expect for CSB^{WT} and CSB$^{K538A\#21}$ at 30 μM menadione where $P = 0.06$. (**D**) Alkaline comet assays measuring SSBs after 15 min exposure to H_2O_2 on ice followed by 30 min recovery. (**E**) Same data as in (D), but with circles representing the mean tail moment of a single experiment and horizontal bars representing the means of three independent experiments (± SEM). Statistical significance was determined by one-way ANOVA with Holm–Sidak's multiple comparison test, of the means from three independent experiments, using a single pooled variance; **$P \leq 0.01$. (**F**) H_2O_2 survival assays. Shown are means ± SEM of three independent experiments. An unpaired *t*-test was used to calculate the statistical significance. ***$P \leq 0.001$, ****$P \leq 0.0001$.

Jose, CA, USA) HRP chemiluminescent substrates, exposed to X-ray film, and imaged with a Konica Processor SRX-101A. X-ray films were scanned, and western signals were quantified using ImageQuantTL (V10.0.261, Cytiva, Marlborough, MA, USA).

Antibodies

Primary antibodies used for western blot analysis were rabbit polyclonal anti-CSB (C-terminus) (1:2000, a gift from Dr Weiner, University of Washington), PARP1-C (1:3000, Active Motif, cat no. 39561, Carlsbad, CA, USA) and XRCC1 (1:2000, Novus, cat. no. NBP1-87154, Centennial, CO, USA). Lamin B1 (1:1000, cat. no. 13435) and HPF1 (1:1000, cat. no. 90876) were from Cell Signaling Technology, Danvers, MA, USA). CTCF (1:2000, cat. no. 07–729), GAPDH (1:10000, cat. no. MAB374) antibodies and the pan ADP-ribose-binding reagent (1:1000, cat. no. MABE1016) were from EMD Millipore (Burlington, MA, USA). Secondary antibodies used were HRP-conjugated goat anti-rabbit IgG (1:10 000, Pierce, cat. no. 31460, Rockford, IL, USA) and HRP-conjugated goat anti-mouse (IgG + IgM) (1:10 000, Jackson Laboratory, cat. no. 115-035-044, Bar Harbor, ME, USA).

RESULTS

CSB regulates SSBR in an ATP-dependent manner

To study the role of CSB in SSBR, we used alkaline comet assays to directly measure DNA lesions that are strand breaks and alkali-labile sites (e.g. apurinic/apyrimidinic sites), which we collectively refer to as SSBs (42) (Figure 1). We first used varying amounts of menadione to create oxidative DNA lesions. After a 1-hour treatment, cells were subjected to alkaline comet assays to measure DNA breaks (Figure 1A). Relative levels of DNA lesions are expressed as 'tail moment' (43). Each dot in Figure 1A represents the tail moment of a single cell, and each column of dots representing a single experiment. 100–150 cells were scored per experiment. Significantly more DNA lesions were left unrepaired in CSB^{null} cells (red) as compared to CSB^{WT} cells (blue) after treating with 10 μM and 30 μM menadione, providing direct evidence that CSB regulates SSBR. After treating cells with 100 μM menadione for 1 hour, similar

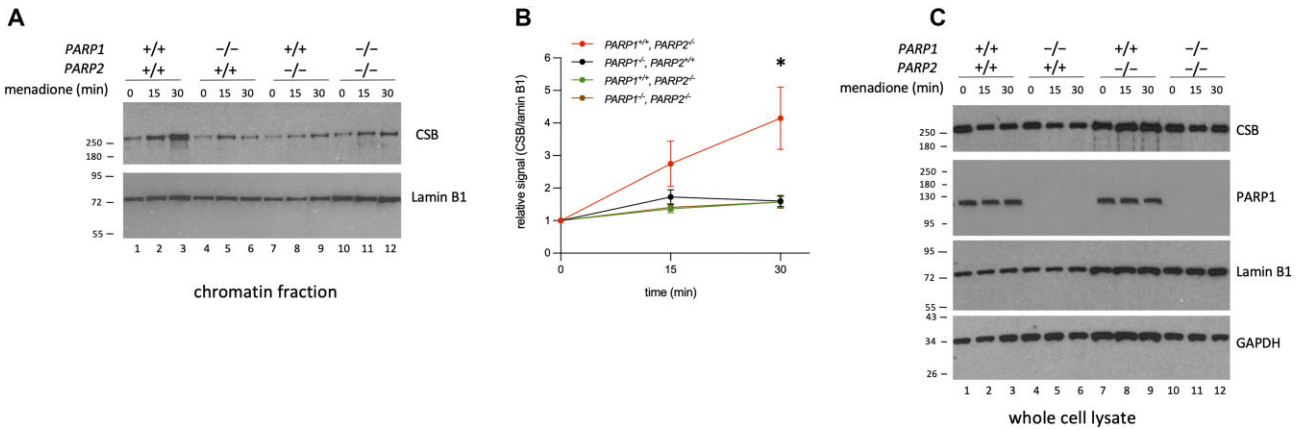

Figure 2. PARP1 and PARP2 recruit CSB to oxidized chromatin. (**A**) Representative western blot of chromatin-enriched protein fractions isolated from the indicated cell lines at different times after menadione treatment. Lamin B1 was used as a loading control. (**B**) Quantification of data shown in (A). CSB signals were normalized with the Lamin B1 loading control, and changes in CSB abundance after treatment were determined relative to no treatment (time 0). Shown are means ± SEM of three independent experiment. Statistical significance was determined using one-way ANOVA with Holm-Sidak's multiple comparison test, of the means, using a single pooled variance; $*P \leq 0.05$. (**C**) Western blot analysis of whole cell lysates. No significant change in total CSB levels occurred over the course of treatment (variation was <30% in each cell line).

amounts of DNA lesions were left unrepaired in cells with or without CSB, suggesting that this treatment generated more DNA damage than the DNA-repair mechanism can accommodate.

Previously, we showed that the association of CSB with oxidized chromatin occurs independently of its ATPase activity (38). Here we asked whether the ATPase activity of CSB is required for its function in SSBR. Using two independent cell lines stably expressing an ATPase-defective CSB mutant (CSB^{K538A}), we found that similar levels of SSBs remained in these cells after 1-h treatments with either 10 or 30 μM menadione as compared to CSB^{null} cells, indicating that CSB promotes SSBR in an ATP-dependent manner (Figure 1A, B). To determine if the ATPase activity of CSB is critical to the viability of oxidatively stressed cells, we performed cell survival assays. As shown in Figure 1C, while wild-type CSB expression in CSB^{null} cells increased their resistance to oxidative stress, the CSB derivative defective for ATP hydrolysis failed to complement the decreased viability. This result demonstrates that the ATPase activity of CSB is critical to cell survival after oxidative stress induced by menadione.

We next used alkaline comet assays to dissect the role of CSB in SSBR. Both menadione and H_2O_2 can produce hydroxyl radicals through the Fenton reaction and that are responsible for most of the DNA damage caused by oxidative stress. However, because of redox cycling, hydroxyl radicals are continuously generated by menadione (44), which is not the case for H_2O_2 treatment, as ROS levels rapidly drop after H_2O_2 removal. Accordingly, to dissect further the function of CSB in DNA repair using alkaline comet assays, H_2O_2 was used as the ROS source. We determined that under our assay conditions, 50 μM H_2O_2 treatment for 15 min on ice permitted completion of most if not all DNA repair within 30 min after recovery at 37°C. Shown in Figure 1D are results from alkaline comet assay, with each dot representing the tail moment of an individual cell and each column of dots representing a single experiment. We also show these data in Figure 1E as circles representing the mean tail moment of a single experiment, with horizontal bars representing the means of the three independent experiments (±SEM).

As shown in Figure 1D and E, no significant difference in the basal level of SSBs was observed between CSB^{null} and CSB^{WT} cells. After treating cells with 50 μM hydrogen peroxide for 15 min on ice, we detected a significant increase in DNA damage with no statistical difference between these two cells lines. Strikingly, after allowing cells to repair DNA in fresh medium at 37°C for 30 min, significantly more damage was left unrepaired in CSB^{null} cells (red) as compared to CSB^{WT} cells (blue), validating our results using menadione (Figure 1A) and confirming that CSB regulates SSBR. Importantly, the level of DNA damage remaining in CSB^{WT} cells after recovery was close to that in untreated CSB^{WT} cells, indicating that the repair of oxidative DNA damage is largely completed within 30 min.

Using the two independent cell lines stably expressing an ATPase-defective CSB mutant (CSB^{K538A}), we found that similar levels of SSBs remained in these cells after 30 min of repair as compared to CSB^{null} cells. These results again demonstrate that CSB promotes SSBR in an ATP-dependent manner. Consistent to our finding using menadione, the CSB derivative defective for ATP hydrolysis failed to complement the decreased viability associated with loss-of-CSB function in the presence of H_2O_2. These results confirm that the ATPase activity of CSB is critical to cell survival during oxidative stress. In summary, treating cells with menadione or hydrogen peroxide generates similar responses in both DNA repair and cell survival assays.

PARP1 and PARP2 recruit CSB to oxidatively damaged chromatin in RPE-1 cells

Previously, we showed that CSB is recruited to chromatin during menadione-induced oxidative stress in fibroblasts, and that PARP1 plays a role in regulating this

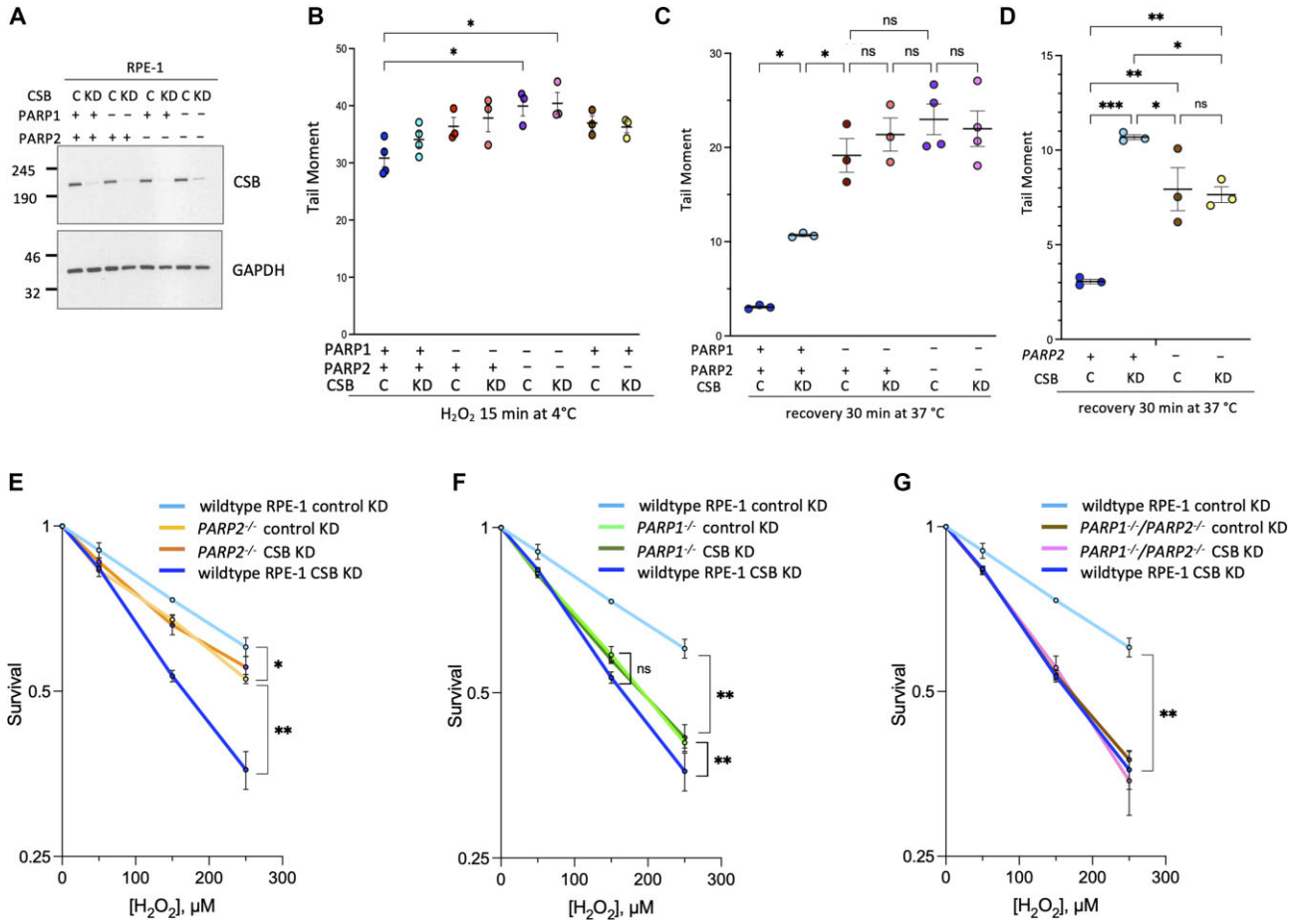

Figure 3. CSB cooperates with PARP1 and PARP2 in oxidative DNA-damage repair. (A–C) SSBs measured by alkaline comet assays in different RPE-1 cell lines with and without CSB KD. Each circle represents the mean from 100–150 cells counted in one experiment. Shown are means ± SEM ($n = 3$ or 4 independent experiments). (**A**) SSBs measured after 15-min H_2O_2 treatment on ice in cells with or without shRNA-mediated CSB KD. Cells expressing a non-targeting shRNA are labeled as control 'C'. Cells expressing an shRNA targeting CSB are labeled as knockdown 'KD'. (**B**) SSBs measured in wildtype RPE-1, *PARP1*$^{-/-}$, and *PARP1*$^{-/-}$/*PARP2*$^{-/-}$ double KO cells after 30-min recovery in fresh medium. (**C**) SSBs measured in *PARP2*$^{-/-}$ cells after 30-min recovery. Wildtype RPE-1 cell data were replotted from (B) to separate *PARP2*$^{-/-}$ from *PARP1*$^{-/-}$ results for clarity. (**D**) Representative western blot showing CSB KD levels in the different RPE-1 cell lines. (E–G) H_2O_2 survival assays. The same survival data from wildtype RPE-1 cells expressing a control KD or CSB shRNA were used in all three panels. Shown are means ± SEM of three independent experiments. An unpaired *t*-test was used to calculate the statistical significance (*:$P \leq 0.05$, **$P \leq 0.01$). (**E**) *PARP2*$^{-/-}$ cells expressing control or CSB-targeting shRNA. (**F**) *PARP1*$^{-/-}$ cells expressing control or CSB-targeting shRNA. (**G**) *PARP1*$^{-/-}$/*PARP2*$^{-/-}$ cells expressing control or CSB-targeting shRNA.

recruitment (37,38). Here, we used the near diploid retinal pigment epithelial (RPE-1) cells that have null mutations engineered into the *PARP1*, *PARP2* or both *PARP1* and *PARP2* genes via the CRISPR/Cas9 system, to examine the individual and collective impact of PARP1 and PARP2 on CSB recruitment to oxidatively damaged chromatin (6). Using chromatin fractionation followed by western blot analysis, we detected a menadione-induced increase in the level of CSB co-fractionating with chromatin in wildtype RPE-1 cells (Figure 2A, B) (22,45). This menadione-induced CSB-chromatin association was attenuated in *PARP1*$^{-/-}$ and *PARP2*$^{-/-}$ cells as well as in *PARP1*$^{-/-}$/ *PARP2* $^{-/-}$ cells (Figure 2A, B). The observed increase of CSB in the chromatin fractions did not result from changes in total CSB levels, as CSB protein levels remained constant under all conditions and in all cell lines assayed (variations were <30%, Figure 2C). These observations reveal that both PARP1 and PARP2 contribute to the recruitment of CSB to oxidatively damaged chromatin.

CSB works in SSBR-mediated by PARP1 and PARP2

We next sought to determine if CSB contributes to PARP1- and PARP2-mediated SSBR by performing alkaline comet assays using the RPE-1 cell line and its PARP1/2 null derivatives. CSB levels were reduced in these cell lines using shRNA-mediated RNA interference (Figure 3A). As shown in Figure 3B, after cells were incubated with H_2O_2 on ice for 15 min, DNA damage accumulated in the wildtype RPE-1, *PARP1*$^{-/-}$, *PARP2*$^{-/-}$ and the *PARP1*$^{-/-}$/*PARP2*$^{-/-}$ double knockout (KO) cell lines, with the levels of damage in the double KO line modestly, but significantly, elevated as compared to the wildtype RPE-1 line. This observation is consistent with the notion that PARP1 and PARP2 have overlapping functions, and when both proteins are absent, a decrease in oxidative DNA-lesion repair is detectable even within the 15 min treatment with 50 μM H_2O_2 on ice. A reduction in CSB level had no further impact on damage accumulation during the 15 min H_2O_2 treatment.

After recovery for 30 min, DNA repair was greatly impaired in the *PARP1*$^{-/-}$ and *PARP1*$^{-/-}$/*PARP2*$^{-/-}$ cell lines as compared to the wildtype RPE-1 cells (Figure 3C). Similar to the CSB^{null} fibroblast cell line, shRNA-mediated CSB KD in the wildtype-RPE-1 epithelial cell line also reduced DNA repair (Figures 3C and 1E). Since reducing CSB levels in the PARP1 KO cell lines did not exacerbate the DNA repair defect, this result suggests that CSB and PARP1 function in the same repair pathway (Figure 3C).

Given that PARP2 accounts for ∼10–20% of the cellular PARylation activity induced by DNA breaks (6,7), we next sought to determine if the repair of oxidative DNA damage mediated by PARP2 is impacted by loss of CSB. As anticipated, DNA repair was less efficient in *PARP2*$^{-/-}$ cells as compared to wildtype RPE-1 cells (Figure 3D, compare brown to dark blue), but less severe than the defect observed in *PARP1*$^{-/-}$ cells (Figure 3C, dark red). Interestingly, more damage remained unrepaired in wildtype RPE-1 cells with CSB KD as compared to *PARP2*$^{-/-}$ cells (Figure 3D, compare light blue to brown). Surprisingly, knocking down CSB in the *PARP2*$^{-/-}$ cells did not exacerbate the DNA repair defect of the *PARP2*$^{-/-}$ cells, but actually lead to a repair defect that was less severe than knocking down CSB in the wildtype RPE-1 cells (Figure 3D, yellow to light blue). In fact, the DNA repair defect resulting from CSB KD in *PARP2*$^{-/-}$ cells was now similar to that of the *PARP2*$^{-/-}$ alone. Therefore, these data reveal that loss of PARP2 suppresses the DNA repair defect caused by reduced CSB levels.

CSB regulates PARP1 and PARP2 function in H_2O_2-treated cells

CSB-deficient cells are hypersensitive to oxidative stress. We next performed cell viability assays to determine the extent to which PARP2 and PARP1 contribute to the hypersensitivity of CSB-deficient cells to hydrogen peroxide (Figure 3E-G, compare dark blue to light blue). We found that wildtype RPE-1 cells with CSB KD were significantly more sensitive to H_2O_2-induced cytotoxicity than the *PARP2*$^{-/-}$ cells (Figure 3E, compare dark blue to yellow). Strikingly, knocking down CSB in *PARP2*$^{-/-}$ did not make *PARP2*$^{-/-}$ cells more sensitive to hydrogen peroxide (Figure 3E, compare orange to yellow), indicating that loss of PARP2 suppresses the hypersensitivity of CSB-deficient cells to H_2O_2 and suggesting that one critical function of CSB in oxidatively stressed cells is to regulate PARP2 activity.

We next determined the extent to which PARP1 contributes to the hypersensitivity of CSB-deficient cells to oxidative stress. As shown in Figure 3F, the *PARP1*$^{-/-}$ cells were slightly less sensitive to H_2O_2 treatment than the wildtype RPE-1 cells with CSB KD (Figure 3F, compare light green to dark blue). Similar to that in *PARP2*$^{-/-}$ cells, knocking down CSB in *PARP1*$^{-/-}$ did not make *PARP1*$^{-/-}$ cells more sensitive to hydrogen peroxide (Figure 3F, compare dark green to light green). Furthermore, loss of PARP1 slightly rescued the inviability of H_2O_2-treated CSB KD cells to the level *of PARP1*$^{-/-}$ cells expressing the control shRNA, which was most apparent at 250 μM H_2O_2, (Figure 3F, compare dark blue to dark green). This result suggests that, in addition to PARP2, CSB may also regulate PARP1 function in oxidatively stressed cells.

Lastly, we found that *PARP1*$^{-/-}$/*PARP2*$^{-/-}$ cells were as sensitive to H_2O_2 as CSB KD cells (Figure 3G, compare brown to blue), and remarkably, knocking down CSB in *PARP1*$^{-/-}$/*PARP2*$^{-/-}$ cells did not further decrease their viability in response to H_2O_2 (Figure 3G, compare brown to pink). Altogether, these results support the hypothesis that CSB works with PARP1 and PARP2 to relieve oxidative stress and suggest that one major CSB function in oxidatively stressed cells is to regulate PARP1 and PARP2 function.

CSB-mediated SSBR is associated with active transcription

Given the well-documented role of CSB in coupling nucleotide excision repair to transcription, we next asked whether transcription impacts CSB-mediated repair of oxidative DNA damage (Figure 4A). We observed no significant difference in DNA damage accumulation after 15-min of H_2O_2 exposure in cells with or without prior treatment with the transcription inhibitor α-amanitin, which prevents ribonucleotide incorporation (Figure 4B). After recovery for 30 min in fresh medium, significantly less damage remained in CSB^{WT} cells as compared to CSB^{null} cells (Figure 4C, compare dark blue to red) without α-amanitin treatment. Transcription inhibition by α-amanitin treatment had an inhibitory effect on DNA damage repair, as the level of damage remaining in CSB^{WT} cells was greater with α-amanitin treatment Figure 4C, compare light blue to dark blue), indicating that transcription is a component of SSBR. Strikingly, α-amanitin treatment abolished the difference in DNA damage levels observed between CSB^{WT} and CSB^{null} cells after recovery (Figure 4C, compare light blue to orange). This result reveals that CSB is required for efficient repair of oxidative DNA damage when cells are actively transcribing DNA, and transcription inhibition bypasses the requirement for CSB permitting partial restoration of SSBR (Figure 4C, compare red to orange).

To complement the above study, we treated cells with the transcription elongation inhibitor 5,6-dichloro-1-beta-D-ribofuranosylbenzimidazole (DRB) (Figure 4D). We found that DRB, like α-amanitin, also dampened oxidative DNA-damage repair (Figure 4D, compare light green to blue) and bypassed CSB function (Figure 4D, compare pink to light green). Together, these results support the hypothesis that oxidative DNA lesion repair contains both transcription-dependent and independent components, and CSB largely regulates oxidative DNA-damage repair in a transcription-dependent manner.

If the increased H_2O_2 sensitivity of CSB^{null} cells relative to CSB^{WT} cells resulted from a defect in the repair of actively transcribed DNA regions, we reasoned that inhibiting transcription in CSB^{WT} cells with α-amanitin would decrease CSB^{WT} cell survival upon oxidative stress to a level similar to untreated CSB^{null} cells. On the other hand, α-amanitin treatment would have no significant impact on the survival of CSB^{null} cells after H_2O_2 treatment. As shown in Supplementary Figure S1, this turned out to be the case: treating CSB^{WT} cells with α-amanitin resulted in an H_2O_2

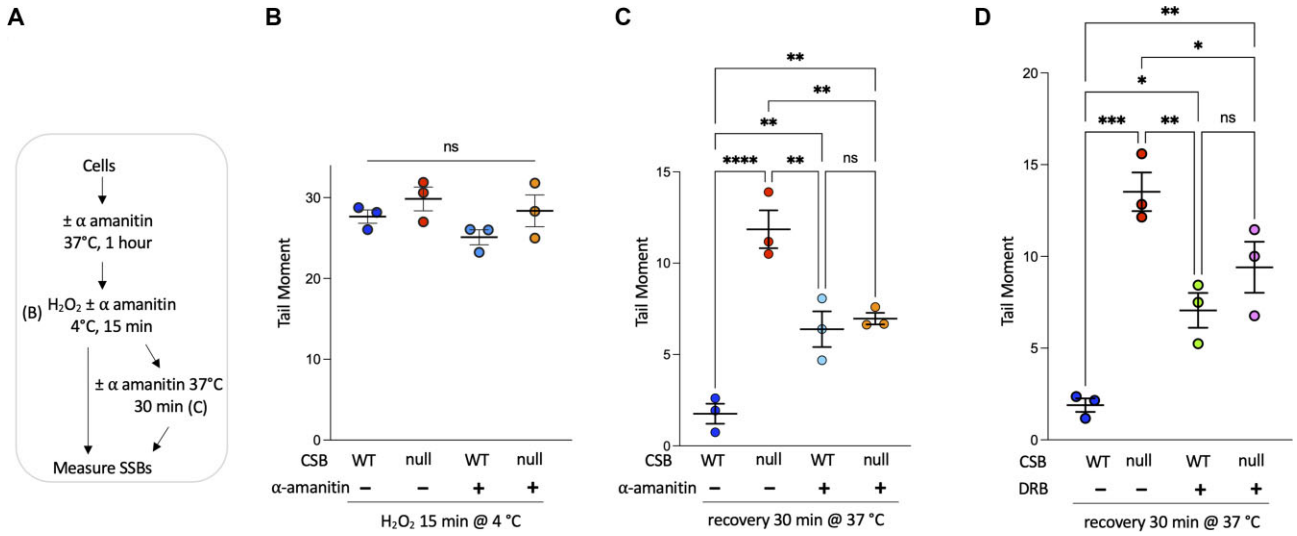

Figure 4. CSB regulates oxidative DNA-damage repair at actively transcribed regions. (**A**) Experimental scheme**.** Effect of α-amanitin treatment on SSB generation (**B**) and SSB repair (**C**) in CSB^{WT} and CSB^{null} cells, measured by alkaline comet assays and expressed as tail moments**.** Each circle represents the mean tail moment of 100–150 cells from one experiment. Shown are the means of three biological replicates ± SEM. Statistical significance was determined using one-way ANOVA with Holm–Sidak's multiple comparison test of the means, using a single pooled variance; $*P \leq 0.05$, $**P \leq 0.01$, $***P \leq 0.001$, $****P \leq 0.0001$. ns: $P > 0.05$. (**D**) Same as (C), except DRB was used.

sensitivity at 50 μM that was similar to CSB^{null} cells, while the sensitivity of CSB^{null} cells with α-amanitin treatment remained unchanged. These results further support the hypothesis that CSB-mediated repair of oxidative DNA damage is associated with actively transcribed DNA regions.

Transcription is a significant component of SSBR mediated by PARP1 and PARP2

Given that PARP1/2 recruit CSB to oxidized chromatin (Figure 2) and CSB-mediated SSBR largely occurs at regions with active transcription (Figure 4), we next examined the extent to which SSBR-mediated by PARP1 and PARP2 is associated with active transcription. If transcription-associated SSBR and PARP1/2-associated SSBR are independent processes, then we would expect that the combined effect of transcription inhibition and loss of PARP1 or PARP2 activity would be additive during SSBR. On the other hand, if transcription-associated SSBR and PARP1/2-associated SSBR are interdependent, then we expect that the combined effect of transcription inhibition and loss of PARP1/2 activity would be similar to their independent effects.

As shown in Figure 5A, transcription inhibition by α-amanitin did not change the level of DNA damage that accumulated in the different RPE cell lines after 15-min H_2O_2 treatment on ice, similar to what we observed in fibroblasts (Figure 4B). Notably, treatment of wildtype RPE-1 cells with α-amanitin resulted in a statistically significant reduction in damage removal, indicating that a fraction of oxidative DNA-damage repair in RPE-1 cells requires active transcription (Figure 5B, middle two data columns). Loss of PARP1 resulted in a substantial increase in the number of unrepaired DNA lesions, and transcription inhibition did not alter the DNA repair defect associated with $PARP1^{-/-}$ cells, indicating that transcription is a significant component of PARP1-mediated SSBR (Figure 5B, left two data columns). Furthermore, when transcription was inhibited, the level of DNA damage left unrepaired in $PARP1^{-/-}$ cells was still significantly greater than that observed in wildtype RPE1 cells treated with α-amanitin (Figure 5B, yellow), indicating that PARP1 also functions in SSBR independent of transcription. These observations, therefore, reveal that PARP1 initiates SSBR regardless of the transcription status.

PARP2 cooperates with CSB in oxidative DNA repair largely at regions with active transcription

Transcription inhibition by α-amanitin treatment also did not change the level of DNA damage remaining in the $PARP2^{-/-}$ cells after recovery (Figure 5B, right two data columns). Remarkably, however, the level of damage remaining in $PARP2^{-/-}$ cells treated with α-amanitin was very similar to that remaining in wildtype RPE-1 cells treated with α-amanitin (yellow), suggesting that the majority of SSBR mediated by PARP2 is associated with active transcription.

To test if CSB participates in transcription-associated SSBR by PARP1 and PARP2, we used alkaline comet assays to examine the impact of transcription inhibition on DNA repair in wildtype RPE-1, $PARP1^{-/-}$ and $PARP2^{-/-}$ cells with and without CSB KD (Figure 5C, D). As observed in fibroblasts (Figure 4C), transcription inhibition by α-amanitin had an inhibitory effect on DNA repair in wildtype RPE-1 cells, but rescued a part of the DNA repair defect associated with CSB KD in wildtype RPE-1 cells (Figure 5D, compare orange to red triangles). While transcription inhibition alone did not significantly alter the DNA repair defect associated with loss of PARP1 (Figure 5D, compare light blue to dark blue circles), transcription inhibition did rescue part of the DNA repair defect associated with

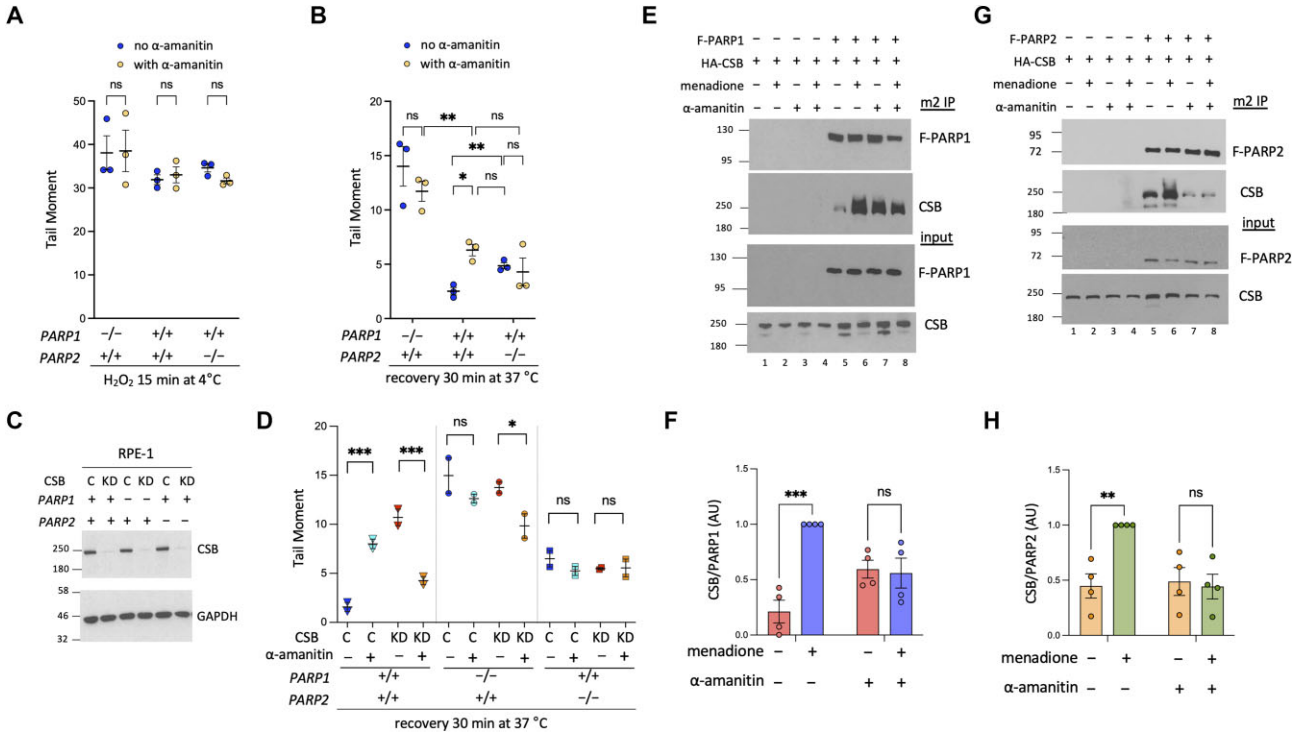

Figure 5. Transcription is a significant component of SSBR-mediated PARP1 and PARP2. (A, B) Alkaline comet assays measuring the effect of α-amanitin on SSB generation and repair in wildtype RPE-1, *PARP1*$^{-/-}$ and *PARP2*$^{-/-}$ cells in response to H_2O_2 treatment. Each circle represents the mean tail moment of 100–150 cells counted in one experiment. Horizontal black bars represent the means ± SEM of three independent experiments. Statistical significance was determined using one-way ANOVA with Holm–Sidak's multiple comparison test. *$P \leq 0.05$, **$P \leq 0.01$, ns: $P > 0.05$. (**A**) SSBs measured in cells treated with 50 μM H_2O_2 for 15 min on ice with or without α-amanitin. (**B**) SSBs measured after 30-min recovery in fresh medium. (**C**) representative western blot showing extent of CSB-mediated KD in the different RPE-1 cell lines. (**D**) Alkaline comet assays measuring the effect of CSB KD on DNA repair with the cell lines and treatments shown in (B). Statistical significance was determined by unpaired *t*-test per row with individual variances computed for each comparison, Holm–Sidak's multiple comparison test. (*$P \leq 0.05$, ***$P \leq 0.01$, ns: $P > 0.05$). (**E**) Representative western blot of a co-immunoprecipitation experiment revealing the effect of menadione and α-amanitin treatment on CSB–PARP1 interactions. (**F**) Quantification of the PARP1-CSB interaction data. Shown are means ± SEM ($n = 4$). Statistical significance was determined by multiple unpaired *t*-test. ***$P \leq 0.001$. (**G**) Same as in (E), except CSB–PARP2 interactions were determined. (**H**) Same as in (F), except CSB–PARP2 interactions were quantified. **$P \leq 0.01$.

CSB KD in PARP1$^{-/-}$ cells (Figure 5D, compare orange to red circles), suggesting that PARP1 is not obligatory for the transcription inhibition-induced bypass of CSB function. However, as shown in Figure 5D (squares), transcription inhibition did not significantly alter the DNA repair defect associated with loss of PAPR2 cells with or without CSB KD. Together, these results further support the hypothesis that PARP2 and CSB work together in oxidative DNA-lesion repair at regions with active transcription.

Oxidative stress enhances the CSB–PARP1/2 interaction and α-amanitin attenuates this enhancement

CSB is known to interact with PARP1, both *in vitro* and in cells (17). We therefore wished to determine if oxidative stress alters this interaction. Flag-tagged PARP1 and HA-tagged CSB were co-transfected into 293T cells. Forty-eight hours post transfection, the cells were treated with menadione for 1 h and immunoprecipitation was carried out using an anti-Flag antibody. As shown in Figure 5E and F, more CSB co-immunoprecipitated with Flag-tagged PARP1 in menadione treated cells, revealing that oxidative stress enhances the interaction of CSB with PARP1. We next tested if transcription inhibition by α-amanitin altered the menadione induced CSB–PARP1 interactions. Strikingly, α-amanitin reduced the menadione-stimulated CSB–PARP1 interaction, strengthening the notions that CSB and PARP1 cooperate in the repair of SSBs and active gene transcription is important for coupling CSB and PARP1 activities in SSBR.

We next determined if CSB interacts with PARP2 and if this interaction is altered by oxidative stress. As shown in Figure 5G and H, PARP2 also interacted with CSB, and this interaction was enhanced by menadione treatment. Remarkably, transcription inhibition also abolished the menadione-induced CSB–PARP2 interaction, supporting the hypothesis that CSB works with PARP2 during oxidative DNA-lesion repair at regions with active transcription.

Histone PARylation factor 1 (HPF1) functions in CSB-mediated SSBR

HPF1 expands the substrate specificity of PARP1/2 to promote serine PARylation, the major PARylation event that occurs during SSBR repair (10,11). Thus, we asked whether HPF1 integrates into CSB-mediated repair of oxidative DNA damage by performing alkaline comet assays

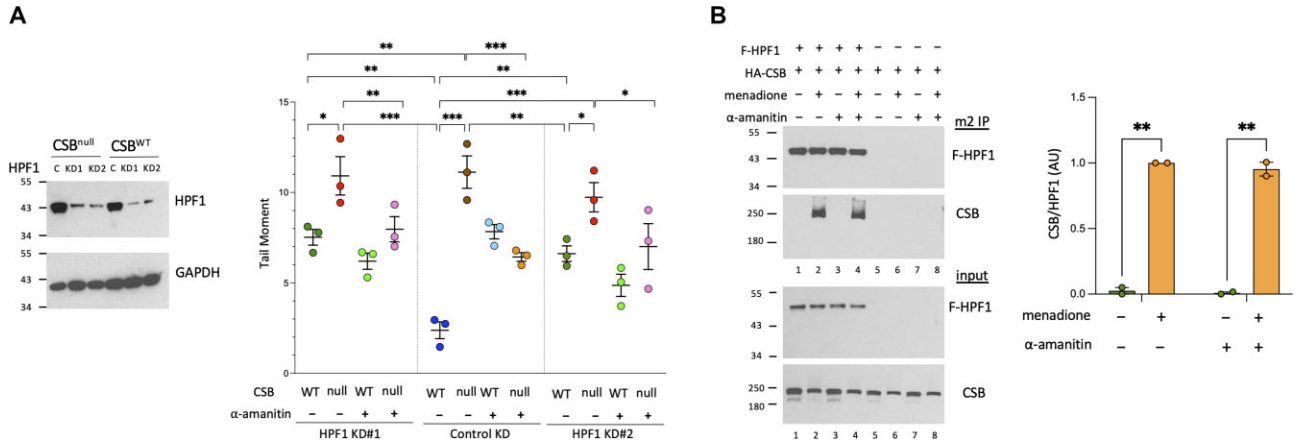

Figure 6. HPF1 contributes to SSBR in CSB- and transcription-dependent manners. (**A**) Representative western blot showing HPF1 protein levels in CSB^{WT} and CSB^{null} cells expressing a control shRNA ('C') and two different shRNAs targeting HPF1 ('KD1' and 'KD2'). (**B**) Alkaline comet assays revealing the impact of HPF1 knockdown in CSB^{WT} and CSB^{null} cells in the presence and absence of α-amanitin. Each circle represents the mean from 100–150 cells counted in one experiment. Shown are means ± SEM ($n = 3$ independent experiments). Statistical significance was determined using one-way ANOVA with Holm–Sidak's multiple comparison test. $*P \leq 0.05$, $**P \leq 0.01$, $***P \leq 0.001$, ns: $P > 0.05$. (**B**) Representative western blot of a co-immunoprecipitation experiment revealing the effect of menadione and α-amanitin treatment on CSB–HPF1 interactions. Quantification of CSB–HPF1 co-immunoprecipitation data from two independent experiments. Shown are means ± SEM ($n = 2$). Statistical significance was determined by multiple unpaired *t*-test. $**P \leq 0.01$.

with cells expressing HPF1-targeting shRNAs. Two different shRNAs targeting HPF1 were used, both showing significant HPF1 KD (Figure 6A). CSB^{WT} cells expressing either HPF1 shRNA displayed a significant DNA-repair defect as compared to CSB^{WT} cells expressing a control shRNA, consistent with the role of HPF1 in DNA-break repair (Figure 6A, compare dark green to dark blue). However, HPF1 KD in CSB^{null} cells did not exacerbate the DNA repair defect associated with loss of CSB alone, revealing that HPF1 activity is a significant component of CSB-mediated oxidative DNA lesion repair (Figure 6A, compare red to brown columns). Interestingly, we found that transcription inhibition by α-amanitin did not exacerbate the DNA repair defect observed in CSB^{WT} cells with HPF1 KD, indicating that transcription is also a significant component of HPF1-mediated SSBR (Figure 6A, dark green to light green). Although α-amanitin rescued the severe DNA repair defect associated with loss of CSB, we did not observe a statistically significant difference in the level of rescue between cells expressing HPF1 shRNA or a control shRNA. Together, these observations indicate that HPF1 participates in CSB-mediated SSBR and likely functions downstream of CSB.

Oxidative stress promotes CSB–HPF1 interaction

Given the association between CSB and HPF1 functions in SSBR (Figure 6A), we next sought to determine if CSB interacts with HPF1. 293T cells were transfected with Flag-tagged HPF1 and HA-tagged CSB. Forty-eight hours post transfection, HPF1-interacting proteins were immunoprecipitated using an anti-Flag antibody. As shown in Figure 6B, Flag-HPF1 interacted with CSB in cells treated with menadione, while no detectable CSB was pulled down by Flag-HPF1 in cells without menadione treatment. Moreover, transcription inhibition by α-amanitin did not significantly alter the menadione induced HPF1 and CSB (Figure 6B).

CSB facilitates recruitment of HPF1 and the SSBR machinery to oxidized chromatin

To dissect the mechanisms by which CSB regulates SSBR-mediated by PARP1/2 at actively transcribed DNA regions, we next examined the recruitment of CSB and components of the SSBR repair machinery to oxidized DNA using chromatin co-fractionation approaches (Figure 7). As shown in Figure 7A and B, CSB demonstrated menadione-induced chromatin association in a time-dependent manner, as we demonstrated previously (25,38). However, treating cells with the transcription inhibitors α-amanitin and DRB, or the PARP inhibitor KU-0058948 that inactivates both PARP1 and PARP2, did not change the kinetics of menadione-induced CSB-chromatin association. These results indicate that transcriptional or PARylation activity have no significant impact on the CSB recruitment to oxidized chromatin. To test if PARP trapping would alter the menadione-induced CSB-chromatin association, we used the pro-retention PARP1 inhibitor EB47 (46). As shown in Supplementary Figure S2, EB47 treatment did not alter the level of CSB that co-fractionated with chromatin after a 30-min menadione treatment.

Like CSB, HPF1 also demonstrated menadione-induced chromatin association (Figure 7A). In addition, treating cells with transcription or PARP inhibitors did not alter the kinetics of menadione induced HPF1-chromatin association (Figure 7A, and supplementary Figure S3A). Strikingly, loss of CSB drastically impeded the recruitment of HPF1 to oxidized chromatin (Figure 7C, D), indicating that CSB plays a critical role in HPF1 recruitment.

Given that histone PARylation is the major function of HPF1, we next sought to determine if CSB impacts

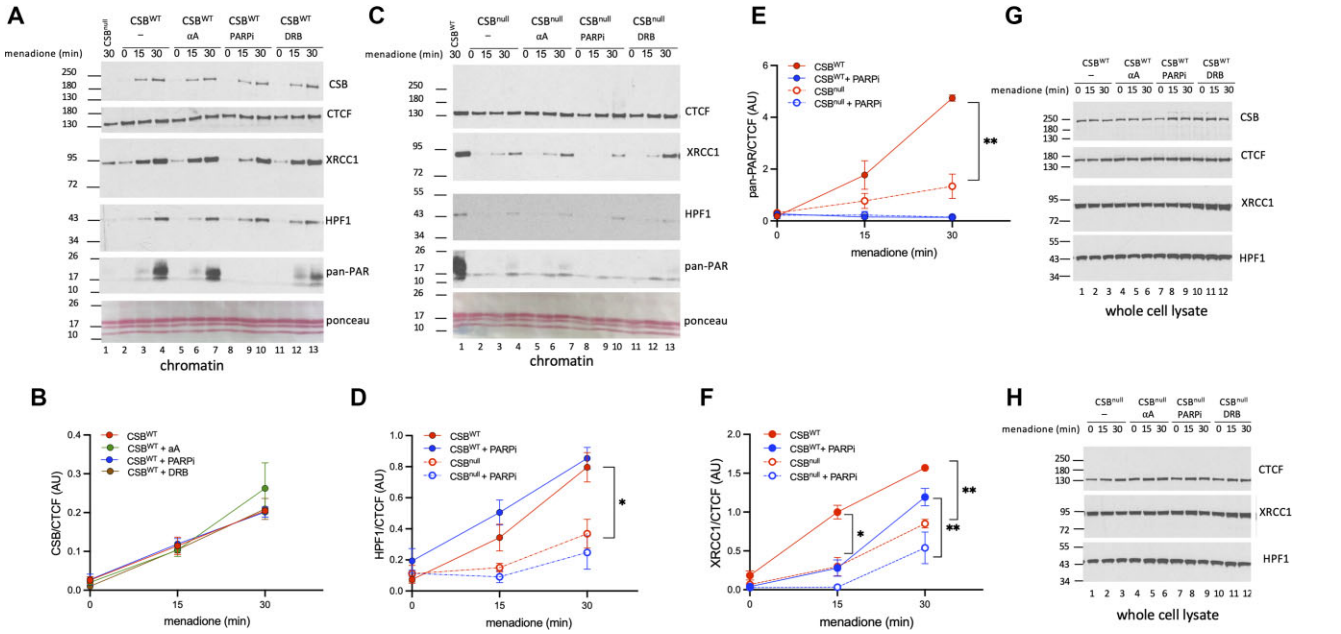

Figure 7. CSB facilitates DNA repair protein recruitment and histone PARylation. (**A**) Representative western blot of chromatin-enriched proteins isolated from CSB^{WT} cells at different times of menadione treatment, in the absence or presence of PARP and transcription inhibitors. (**B**) Plot showing changes in CSB–chromatin association as a function of treatment time. CSB signals were normalized to CTCF signals, which remained largely unchanged. Data were quantified from three independent experiments and plotted as means (± SEM). (**C**) Representative western blot of chromatin-enriched proteins isolated from CSB^{null} cells at different times of menadione treatment, in the absence or presence of PARP and transcription inhibitors. (**D**) Plot showing changes in HPF1-chromatin association in CSB^{WT} and CSB^{null} cells. Data were quantified and normalized as in (B). (**E**) Plot showing changes in PARylation of proteins in the size range of histones, in CSB^{WT} and CSB^{null} cells. (**F**) Plot showing changes in XRCC1-chromatin association in CSB^{WT} and CSB^{null} cells. (**G**) Western blot analysis of total cellular proteins isolated from CSB^{WT} cells under the indicated conditions. (**H**) Western blot analysis of total cellular proteins isolated from CSB^{null} cells under the indicated conditions. Statistical significance was determined unpaired *t*-test. $*P \leq 0.05$ and $**P \leq 0.01$.

histone PARylation by assaying for CSB-mediated effects on poly(ADP-ribose) (PAR) signals in the size range of histone proteins. While we observed a menadione-induced increase in PAR-signal in the size range of histone proteins, this signal was not significantly altered by transcription inhibition through either α-amanitin or DRB treatment (Figure 7A and Supplementary Figure S3B), but it was diminished by a PARP inhibitor (Figure 7A, E, and Supplementary Figure S3B), validating that this PAR signal resulted from PARP1/2 activity. Strikingly, we observed a substantial decrease in histone PARylation in CSB^{null} cells (Figure 7C and E, and supplementary Figure S3B) as compared to CSB^{WT} cells. Again, the remaining PARylation signal was significantly decreased by PARP activity inhibition, while transcription inhibition did not significantly alter this signal. Moreover, loss of CSB also decreased the levels of PARP1/2 autoPARylation (Supplementary Figure S4). Together, these results are consistent with the hypothesis that CSB facilitates the recruitment of HPF1 to oxidized chromatin to promote histone PARylation.

XRCC1 is a scaffolding protein critical for SSBR and is recruited to oxidized chromatin in a PARP1/2 activity-dependent manner. Previously, we showed that CSB also promotes the recruitment of XRCC1 to oxidized chromatin. Here we sought to determine if CSB and PARP1/2 activity are two independent machineries that recruit XRCC1 to oxidized chromatin. As shown in Figure 7A, C and F, and supplementary Figure S3C, the decrease in XRCC1 recruitment resulting from simultaneous loss of the CSB protein and PARP1/2 activity is greater than that from their individual loss. Figure 7G and H reveals that total XRCC1 levels were not significantly altered in whole cell extracts. Therefore, the recruitment of XRCC1 to oxidized chromatin is mediated by both CSB and PARP1/2 activity. Altogether, the results of this study reveal that the CSB chromatin remodeler regulates the repair of oxidative DNA lesions by promoting the recruitment of SSB signaling and repair factors to oxidized chromatin.

DISCUSSION

In this study, we demonstrate that PARP1 and PARP2 recruit CSB to oxidatively damaged DNA (Figure 2) and that CSB is critical for enhancing HPF1 association with oxidized chromatin, which occurs independently of the enzymatic activity of PARP1/2 (Figure 7). Furthermore, our study indicates that CSB is important for the regulation of histone PARylation during SSBR (Figure 7). Using alkaline comet assays, we provide the first direct evidence that the CSB ATP-dependent chromatin remodeler plays a significant role in the repair of SSBs resulting from oxidative stress (Figure 1). Strikingly, the requirement for CSB activity in SSBR is largely bypassed when transcription is inhibited, indicating that SSBR mediated by CSB occurs mostly at actively transcribed DNA regions (Figure 4). Furthermore, while PARP1 can initiate SSBR independently of the local transcription status, we show that transcription inhibition or CSB depletion does not alter the DNA repair defect associated with loss of PARP2, indicating that PARP2 largely initiates SSBR at actively transcribed DNA regions

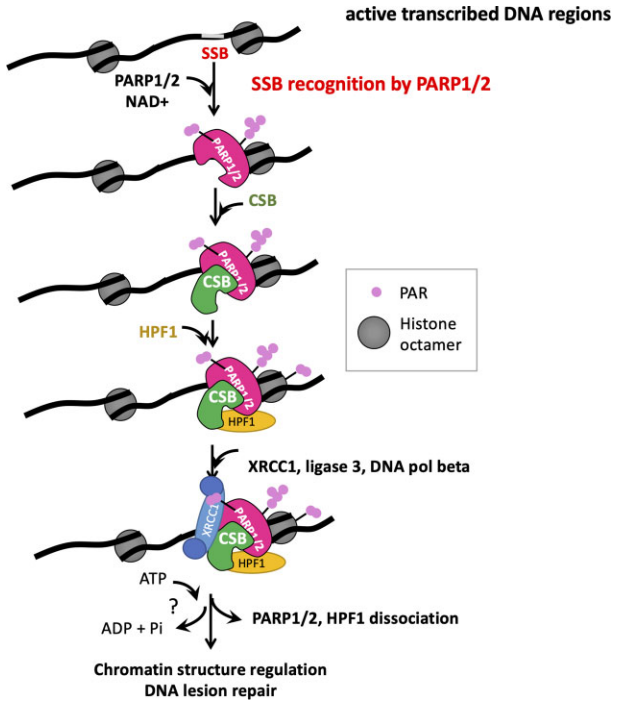

Figure 8. Model for the cooperation of CSB and PARP1/2 in SSBR at actively transcribed DNA regions. SSBs at actively transcribed DNA regions are recognized by PARP1 or PARP2, which then recruit CSB. CSB recruitment does not require ATP hydrolysis by CSB or the PARylation activity of PARP1/2. Once bound, CSB facilitates the recruitment or stabilizes the association of HPF1 with oxidized chromatin, leading to the alteration of the PARP1/2 substrate specificity to include histone serine PARylation. Chromatin-bound CSB also facilitates the recruitment of the SSBR machinery, such as XRCC1 and DNA ligase 3. Execution of SSBR requires the ATP-dependent chromatin remodeling activity of CSB, which may be used to facilitate PARP1/2 dissociation and/or alter chromatin structure at actively transcribed DNA regions to promote efficient repair.

(Figure 5). Our work, therefore, reveals that SSBR employs different regulatory mechanisms at regions of active transcription compared to regions that are not undergoing transcription.

We propose a model that incorporates the roles of PARP1, PARP2, and CSB in the repair of SSBs (Figure 8). First, the binding of PARP1 and PARP2 to SSBs at actively transcribed DNA regions leads to CSB recruitment (Figure 2). CSB recruitment occurs independently of its ATPase activity as well as the PARylation activity of PARP1/PARP2 (Figure 7 and supplementary Figure S2) (38). Once bound, CSB facilitates the recruitment or stabilizes the association of HPF1 with oxidized chromatin, which expands the PARP1/PARP2 substrate targets to include histone serine PARylation. Histone PARylation can lead to chromatin decompaction (47), which may promote CSB-mediated SSBR. Once bound, CSB, along with PARylated PARP1/2, promotes the recruitment of the SSBR factors (Figure 7 and supplementary Figure S3). A limitation of this study is that chromatin-cofractionation experiments do not demonstrate that CSB is recruited to SSBs. Nonetheless, collectively, our results reveal that CSB plays a critical role in the repair of oxidative stress-induced DNA lesions.

Although CSB recruitment to SSBs does not require ATP hydrolysis, we found that the ATP-hydrolysis activity of CSB is required for the execution of SSBR (Figure 1). It remains to be determined how ATP-dependent chromatin remodeling activity of CSB facilitates SSBR. PARP1 and PARP2 bind to SSBs to initiate SSBR but then need to be removed from damaged DNA to allow repair to ensue. Evidence indicates that auto-PARylation leads to the dissociation of PARP proteins from damaged DNA, presumably by electrostatic repulsion (48). However, HPF1 has been shown to decrease the level of PARP1 automodification, and *in vitro* fluorescence polarization experiments reveal that HPF1 decreases the dissociation constant of PARP1 from DNA (49). Together, these observations suggest that additional mechanisms may be needed to promote PARP1/2 dissociation from chromatin. CSB may fulfill this role to promote efficient SSBR at actively transcribed DNA regions. Previously, we found that the loss of PARP1 rescues the hypersensitivity of CSB KD cells to menadione-induced oxidative stress (37). In the present study, we reveal that the loss of PARP1 as well as loss of PARP2 rescue the hypersensitivity of CSB KD cells to H_2O_2 treatment to the levels of $PARP1^{-/-}$ and $PARP2^{-/-}$, respectively (Figure 3). These findings are consistent with a model whereby CSB facilitates PARP1/PARP2 dissociation from chromatin to promote SSBR (Figure 8). Given that loss of PARP2 rescues the severe defect associated with CSB KD to a greater degree than loss of PARP1, this suggests that CSB has a more significant role in regulating PARP2 than PARP1 function during oxidative DNA repair. In the absence of CSB, PARP2 (and PARP1) might have a prolonged residence time at lesions in transcribed DNA region, which would prevent efficient repair.

ATP-dependent chromatin remodelers use ATP as energy to alter DNA/histone contacts. In addition, some chromatin remodelers can also dissociate nonhistone proteins from chromatin (18). Interestingly, the activity of the ALC1 chromatin remodeler is stimulated upon binding to PARylated proteins through its macrodomain (19,50–52). Using live cell imaging and micro-irradiation, ALC1 was shown to dissociate PARP2, but not PARP1, from sites of DNA lesions, and this dissociation occurred in an ATP-dependent manner (19). CSB has been shown to facilitate PARP1 dissociation from DNA *in vitro,* albeit with modest activity (36). The ATP-dependent chromatin remodeling activity of CSB can be significantly enhanced through direct interaction with other proteins, such as the histone chaperones NAP1L1 or NAP1L4 (23). CSB contains a PAR-binding modules (PBM) (35,36) that reside within the NAP1L1/4 binding region (23). It is tempting to speculate that CSB, like ALC1, may also be activated by its interaction with PARylated proteins to promote the removal of PARP1/PARP2 from SSBs, allowing for the efficient repair of transcribed DNA regions.

Using chromatin co-fractionation assays, we found that CSB recruitment to oxidized chromatin still occurs when transcription is inhibited (Figure 7A-B), indicating that CSB-chromatin association largely occurs independent of the transcription status in cells with wildtype PARP1 and PARP2. It remains possible that a fraction of CSB co-fractionating with chromatin is transcription-dependent, but is masked by transcription-independent CSB-chromatin interactions, and the global chromatin approach that we employed does not offer the necessary

resolution. Previously, using CSB ChIP-qPCR, we found that transcription inhibition by α-amanitin and DRB reduced the level of CSB recruitment to the top four menadione-induced CSB binding sites we identified by more than 50% (38), supporting the notion that CSB recruitment to specific genomic regions is transcription dependent. Alternatively, but not mutually exclusive, the recruitment of CSB to oxidized chromatin may be primarily independent of transcription status, but the steps post CSB recruitment are transcription dependent in SSBR. Using laser micro-irradiation in conjunction with a photosensitizer to specifically generate local 8-oxo-7,8-dihydroguanine (8-oxoG) lesions, Menoni *et al.* observed that the recruitment of CSB to these sites is sensitive to transcription inhibition (34). The difference in transcription dependence could be reconciled by the existence of different sensing mechanisms for oxidized guanine versus ROS-induced SSBs: the former requiring CSB interacting with 8-oxoG paused RNA polymerase, as was proposed, and the latter requiring PARP1/2 interactions (Figure 2). However, the results presented in this current study, using PARP1 and PARP2 KO cell lines, clearly demonstrate that efficient CSB recruitment to oxidized chromatin requires the PARP1 and PARP2 proteins but not their activity (Figures 2 and 7 and Supplementary Figure S2) (38). Therefore, it would be interesting to see how loss of PARP1 and PARP2 proteins, as compared to activity inhibition, impact CSB recruitment to laser-generated 8-oxoG lesions.

Why would CSB activity be predominantly needed at SSBs that occurs at actively transcribed DNA regions? When transcription is active, RNA polymerase II constrains chromatin movement, exemplified by liquid droplet formation of transcription-related factors or classic transcription factories. Transcription inhibition can release this constraint, causing partial chromatin reorganization and dispersal of some chromosomal domains (53,54). Such chromatin reorganization might bypass the need for CSB in transcription-associated SSBR. Alternatively, transcription inhibition may activate another DNA repair mechanism upon oxidative stress. Indeed, transcription inhibition has been shown to potentiate other DNA repair mechanisms (55–57). For example, transcription inhibition by DRB potentiates recombinational repair of UV lesions. To determine if this might be the case for H_2O_2 created DNA lesions, we probed for γH2AX accumulation using our experimental conditions (Figure 4C, D); however, we did not observe any change in γH2AX levels within 2 h of the onset of oxidative stress. Stoimenov *et al.* observed increased γH2AX foci after 24-h treatment with 20 μM DRB (57). In our assays, however, cells were only treated with DRB for <2 h. Future experiments with different markers for DNA repair machinery might provide insights into alternative DNA repair mechanisms that might be activated by transcription inhibition and bypass the requirement for CSB in transcription-associated oxidative DNA lesion repair.

DATA AVAILABILITY

The databases used in this work are publicly available (GenBank) or indicated within the text.

SUPPLEMENTARY DATA

Supplementary Data are available at NAR Online.

ACKNOWLEDGEMENTS

We thank Mary Ann Osley for her careful reading and comments on this manuscript. We are grateful to Laurie Hudson for providing the comet assay equipment and analysis tools. We also thank Seema Khattri Bhandari, Annahita Sallmyr of the Tomkinson lab for reagents and technical support. We thank Shane McQueen for his help with some western blot analyses.

Author contributions: Conceptualization, R.J.L. R.B., A.T. and H.-Y.F.; methodology, R.J.L., R.B., K.L.C., A.T. and H.-Y.F.; validation, R.J.L., R.B. and H.-Y.F.; formal analysis, R.J.L., R.B. and H.-Y.F.; investigation, R.J.L., R.B. and H.-Y.F.; resources, R.J.L., R.B., K.L.C., A.T. and H.-Y.F.; data curation, R.J.L., R.B. and H.-Y.F.; writing—original draft preparation, R.J.L., R.B. and H.-Y.F.; writing—review and editing, R.J.L., R.B., K.L.C., A.T. and H.-Y.F.; visualization, R.J.L., R.B. and H.-Y.F.; supervision, H.-Y.F.; project administration, H.-Y.F.; funding acquisition, H.-Y.F. All authors have read and agreed to the published version of the manuscript.

FUNDING

Cancer Center Support Grant [P30CA118100]; National Institutes of Health [GM115888 to H.-Y.F., ES012512 to A.E.T, ES030993 to L.G.H.]. Funding for open access charge: National Institutes of Health (P30CA118100).
Conflict of interest statement. None declared.

REFERENCES

1. Ames,B.N., Shigenaga,M.K. and Hagen,T.M. (1993) Oxidants, antioxidants, and the degenerative diseases of aging. *Proc. Natl. Acad. Sci. U.S.A.*, **90**, 7915–7922.
2. Lindahl,T., Satoh,M.S., Poirier,G.G. and Klungland,A. (1995) Post-translational modification of poly(ADP-ribose) polymerase induced by DNA strand breaks. *Trends Biochem. Sci*, **20**, 405–411.
3. Caldecott,K.W. (2007) Mammalian single-strand break repair: mechanisms and links with chromatin. *DNA Repair (Amst.)*, **6**, 443–453.
4. Ray Chaudhuri,A. and Nussenzweig,A. (2017) The multifaceted roles of PARP1 in DNA repair and chromatin remodelling. *Nat. Rev. Mol. Cell Biol.*, **18**, 610–621.
5. Kumar,N., Raja,S. and Van Houten,B. (2020) The involvement of nucleotide excision repair proteins in the removal of oxidative DNA damage. *Nucleic Acids Res.*, **48**, 11227–11243.
6. Hanzlikova,H., Gittens,W., Krejcikova,K., Zeng,Z. and Caldecott,K.W. (2017) Overlapping roles for PARP1 and PARP2 in the recruitment of endogenous XRCC1 and PNKP into oxidized chromatin. *Nucleic Acids Res.*, **45**, 2546–2557.
7. Ame,J.C., Rolli,V., Schreiber,V., Niedergang,C., Apiou,F., Decker,P., Muller,S., Hoger,T., Menissier-de Murcia,J. and de Murcia,G. (1999) PARP-2, A novel mammalian DNA damage-dependent poly(ADP-ribose) polymerase. *J. Biol. Chem.*, **274**, 17860–17868.
8. Suskiewicz,M.J., Zobel,F., Ogden,T.E.H., Fontana,P., Ariza,A., Yang,J.C., Zhu,K., Bracken,L., Hawthorne,W.J., Ahel,D. *et al.* (2020) HPF1 completes the PARP active site for DNA damage-induced ADP-ribosylation. *Nature*, **579**, 598–602.
9. Palazzo,L., Leidecker,O., Prokhorova,E., Dauben,H., Matic,I. and Ahel,I. (2018) Serine is the major residue for ADP-ribosylation upon DNA damage. *Elife*, **7**, e34334.

10. Bonfiglio,J.J., Fontana,P., Zhang,Q., Colby,T., Gibbs-Seymour,I., Atanassov,I., Bartlett,E., Zaja,R., Ahel,I. and Matic,I. (2017) Serine ADP-ribosylation depends on HPF1. *Mol. Cell*, **65**, 932–940.
11. Gibbs-Seymour,I., Fontana,P., Rack,J.G.M. and Ahel,I. (2016) HPF1/C4orf27 is a PARP-1-interacting protein that regulates PARP-1 ADP-ribosylation activity. *Mol. Cell*, **62**, 432–442.
12. Pandey,N. and Black,B.E. (2021) Rapid detection and signaling of DNA damage by PARP-1. *Trends Biochem. Sci*, **46**, 744–757.
13. Lehmann,A.R. (1982) Three complementation groups in Cockayne syndrome. *Mutat. Res.*, **106**, 347–356.
14. Nance,M.A. and Berry,S.A. (1992) Cockayne syndrome: review of 140 cases. *Am. J. Med. Genet.*, **42**, 68–84.
15. Troelstra,C., van Gool,A., de Wit,J., Vermeulen,W., Bootsma,D. and Hoeijmakers,J.H. (1992) ERCC6, a member of a subfamily of putative helicases, is involved in Cockayne's syndrome and preferential repair of active genes. *Cell*, **71**, 939–953.
16. Citterio,E., Van Den Boom,V., Schnitzler,G., Kanaar,R., Bonte,E., Kingston,R.E., Hoeijmakers,J.H. and Vermeulen,W. (2000) ATP-dependent chromatin remodeling by the Cockayne syndrome B DNA repair-transcription-coupling factor. *Mol. Cell. Biol.*, **20**, 7643–7653.
17. Thorslund,T., von Kobbe,C., Harrigan,J.A., Indig,F.E., Christiansen,M., Stevnsner,T. and Bohr,V.A. (2005) Cooperation of the Cockayne syndrome group B protein and poly(ADP-ribose) polymerase 1 in the response to oxidative stress. *Mol. Cell. Biol.*, **25**, 7625–7636.
18. Clapier,C.R., Iwasa,J., Cairns,B.R. and Peterson,C.L. (2017) Mechanisms of action and regulation of ATP-dependent chromatin-remodelling complexes. *Nat. Rev. Mol. Cell Biol.*, **18**, 407–422.
19. Blessing,C., Mandemaker,I.K., Gonzalez-Leal,C., Preisser,J., Schomburg,A. and Ladurner,A.G. (2020) The oncogenic helicase ALC1 regulates PARP inhibitor potency by trapping PARP2 at DNA breaks. *Mol. Cell*, **80**, 862–875.
20. Auble,D.T., Wang,D., Post,K.W. and Hahn,S. (1997) Molecular analysis of the SNF2/SWI2 protein family member MOT1, an ATP-driven enzyme that dissociates TATA-binding protein from DNA. *Mol. Cell. Biol.*, **17**, 4842–4851.
21. Lake,R.J. and Fan,H.Y. (2013) Structure, function and regulation of CSB: a multi-talented gymnast. *Mech. Ageing Dev.*, **134**, 202–211.
22. Lake,R.J., Geyko,A., Hemashettar,G., Zhao,Y. and Fan,H.Y. (2010) UV-induced association of the CSB remodeling protein with chromatin requires ATP-dependent relief of N-terminal autorepression. *Mol. Cell*, **37**, 235–246.
23. Cho,I., Tsai,P.F., Lake,R.J., Basheer,A. and Fan,H.Y. (2013) ATP-dependent chromatin remodeling by Cockayne syndrome protein B and NAP1-like histone chaperones is required for efficient transcription-coupled DNA repair. *PLoS Genet.*, **9**, e1003407.
24. Boetefuer,E.L., Lake,R.J. and Fan,H.Y. (2018) Mechanistic insights into the regulation of transcription and transcription-coupled DNA repair by Cockayne syndrome protein B. *Nucleic Acids Res.*, **46**, 7471–7479.
25. Lake,R.J., Boetefuer,E.L., Won,K.J. and Fan,H.Y. (2016) The CSB chromatin remodeler and CTCF architectural protein cooperate in response to oxidative stress. *Nucleic Acids Res.*, **44**, 2125–2135.
26. Khobta,A. and Epe,B. (2013) Repair of oxidatively generated DNA damage in Cockayne syndrome. *Mech. Ageing Dev.*, **134**, 253–260.
27. Pascucci,B., Lemma,T., Iorio,E., Giovannini,S., Vaz,B., Iavarone,I., Calcagnile,A., Narciso,L., Degan,P., Podo,F. *et al.* (2012) An altered redox balance mediates the hypersensitivity of Cockayne syndrome primary fibroblasts to oxidative stress. *Aging Cell*, **11**, 520–529.
28. Slyskova,J., Sabatella,M., Ribeiro-Silva,C., Stok,C., Theil,A.F., Vermeulen,W. and Lans,H. (2018) Base and nucleotide excision repair facilitate resolution of platinum drugs-induced transcription blockage. *Nucleic Acids Res.*, **46**, 9537–9549.
29. Yu,A., Fan,H.Y., Liao,D., Bailey,A.D. and Weiner,A.M. (2000) Activation of p53 or loss of the Cockayne syndrome group B repair protein causes metaphase fragility of human U1, U2, and 5S genes. *Mol. Cell*, **5**, 801–810.
30. Pavelitz,T., Bailey,A.D., Elco,C.P. and Weiner,A.M. (2008) Human U2 snRNA genes exhibit a persistently open transcriptional state and promoter disassembly at metaphase. *Mol. Cell. Biol.*, **28**, 3573–3588.
31. Hanawalt,P.C. and Spivak,G. (2008) Transcription-coupled DNA repair: two decades of progress and surprises. *Nat. Rev. Mol. Cell Biol.*, **9**, 958–970.
32. van der Weegen,Y., Golan-Berman,H., Mevissen,T.E.T., Apelt,K., Gonzalez-Prieto,R., Goedhart,J., Heilbrun,E.E., Vertegaal,A.C.O., van den Heuvel,D., Walter,J.C. *et al.* (2020) The cooperative action of CSB, CSA, and UVSSA target TFIIH to DNA damage-stalled RNA polymerase II. *Nat. Commun.*, **11**, 2104.
33. Andrade,L.N., Nathanson,J.L., Yeo,G.W., Menck,C.F. and Muotri,A.R. (2012) Evidence for premature aging due to oxidative stress in iPSCs from Cockayne syndrome. *Hum. Mol. Genet.*, **21**, 3825–3834.
34. Menoni,H., Hoeijmakers,J.H. and Vermeulen,W. (2012) Nucleotide excision repair-initiating proteins bind to oxidative DNA lesions in vivo. *J. Cell Biol.*, **199**, 1037–1046.
35. Pleschke,J.M., Kleczkowska,H.E., Strohm,M. and Althaus,F.R. (2000) Poly(ADP-ribose) binds to specific domains in DNA damage checkpoint proteins. *J. Biol. Chem.*, **275**, 40974–40980.
36. Scheibye-Knudsen,M., Mitchell,S.J., Fang,E.F., Iyama,T., Ward,T., Wang,J., Dunn,C.A., Singh,N., Veith,S., Hasan-Olive,M.M. *et al.* (2014) A high-fat diet and NAD(+) activate Sirt1 to rescue premature aging in cockayne syndrome. *Cell Metab.*, **20**, 840–855.
37. Lake,R.J., Bilkis,R. and Fan,H.Y. (2022) Dynamic interplay between Cockayne syndrome protein B and poly(ADP-ribose) polymerase 1 during oxidative DNA damage repair. *Biomedicines*, **10**, 361.
38. Boetefuer,E.L., Lake,R.J., Dreval,K. and Fan,H.Y. (2018) Poly(ADP-ribose) polymerase 1 (PARP1) promotes oxidative stress-induced association of Cockayne syndrome group B protein with chromatin. *J. Biol. Chem.*, **293**, 17863–17874.
39. Lake,R.J., Boetefuer,E.L., Tsai,P.F., Jeong,J., Choi,I., Won,K.J. and Fan,H.Y. (2014) The sequence-specific transcription factor c-Jun targets Cockayne syndrome protein B to regulate transcription and chromatin structure. *PLoS Genet.*, **10**, e1004284.
40. Langelier,M.-F., Steffen,J.D., Riccio,A.A., McCauley,M. and Pascal,J.M. (2017) In: Tulin,A.V. (ed). *Poly(ADP-Ribose) Polymerase: Methods and Protocols*. Springer, NY, pp. 431–444.
41. Liszczak,G., Diehl,K.L., Dann,G.P. and Muir,T.W. (2018) Acetylation blocks DNA damage-induced chromatin ADP-ribosylation. *Nat. Chem. Biol.*, **14**, 837–840.
42. Adamowicz,M., Hailstone,R., Demin,A.A., Komulainen,E., Hanzlikova,H., Brazina,J., Gautam,A., Wells,S.E. and Caldecott,K.W. (2021) XRCC1 protects transcription from toxic PARP1 activity during DNA base excision repair. *Nat. Cell Biol.*, **23**, 1287–1298.
43. Moller,P., Azqueta,A., Boutet-Robinet,E., Koppen,G., Bonassi,S., Milic,M., Gajski,G., Costa,S., Teixeira,J.P., Costa Pereira,C. *et al.* (2020) Minimum Information for Reporting on the Comet Assay (MIRCA): recommendations for describing comet assay procedures and results. *Nat. Protoc.*, **15**, 3817–3826.
44. Aherne,S.A. and O'Brien,N.M. (2000) Mechanism of protection by the flavonoids, quercetin and rutin, against tert-butylhydroperoxide- and menadione-induced DNA single strand breaks in Caco-2 cells. *Free Radic. Biol. Med.*, **29**, 507–514.
45. Boetefuer,E.L., Lake,R.J., Dreval,K. and Fan,H.Y. (2018) Poly(ADP-ribose) polymerase 1 (PARP1) promotes oxidative stress-induced association of Cockayne syndrome group B protein with chromatin. *J. Biol. Chem.*, **293**, 17863–17874.
46. Zandarashvili,L., Langelier,M.F., Velagapudi,U.K., Hancock,M.A., Steffen,J.D., Billur,R., Hannan,Z.M., Wicks,A.J., Krastev,D.B., Pettitt,S.J. *et al.* (2020) Structural basis for allosteric PARP-1 retention on DNA breaks. *Science*, **368**, eaax6367.
47. Poirier,G.G., de Murcia,G., Jongstra-Bilen,J., Niedergang,C. and Mandel,P. (1982) Poly(ADP-ribosyl)ation of polynucleosomes causes relaxation of chromatin structure. *Proc. Natl. Acad. Sci. U.S.A.*, **79**, 3423–3427.
48. Satoh,M.S. and Lindahl,T. (1992) Role of poly(ADP-ribose) formation in DNA repair. *Nature*, **356**, 356–358.
49. Langelier,M.F., Billur,R., Sverzhinsky,A., Black,B.E. and Pascal,J.M. (2021) HPF1 dynamically controls the PARP1/2 balance between initiating and elongating ADP-ribose modifications. *Nat. Commun.*, **12**, 6675.
50. Bacic,L., Gaullier,G., Sabantsev,A., Lehmann,L.C., Brackmann,K., Dimakou,D., Halic,M., Hewitt,G., Boulton,S.J. and Deindl,S. (2021)

Structure and dynamics of the chromatin remodeler ALC1 bound to a PARylated nucleosome. *Elife*, **10**, e71420.
51. Lehmann,L.C., Hewitt,G., Aibara,S., Leitner,A., Marklund,E., Maslen,S.L., Maturi,V., Chen,Y., van der Spoel,D., Skehel,J.M. *et al.* (2017) Mechanistic insights into autoinhibition of the oncogenic chromatin remodeler ALC1. *Mol. Cell*, **68**, 847–859.
52. Ahel,D., Horejsí,Z., Wiechens,N., Polo,S.E., Garcia-Wilson,E., Ahel,I., Flynn,H., Skehel,M., West,S.C., Jackson,S.P. *et al.* (2009) Poly(ADP-ribose)-dependent regulation of DNA repair by the chromatin remodeling enzyme ALC1. *Science*, **325**, 1240–1243.
53. Nagashima,R., Hibino,K., Ashwin,S.S., Babokhov,M., Fujishiro,S., Imai,R., Nozaki,T., Tamura,S., Tani,T., Kimura,H. *et al.* (2019) Single nucleosome imaging reveals loose genome chromatin networks via active RNA polymerase II. *J. Cell Biol.*, **218**, 1511–1530.
54. Haaf,T. and Ward,D.C. (1996) Inhibition of RNA polymerase II transcription causes chromatin decondensation, loss of nucleolar structure, and dispersion of chromosomal domains. *Exp. Cell. Res.*, **224**, 163–173.
55. Chavez,S., Beilharz,T., Rondon,A.G., Erdjument-Bromage,H., Tempst,P., Svejstrup,J.Q., Lithgow,T. and Aguilera,A. (2000) A protein complex containing Tho2, Hpr1, Mft1 and a novel protein, Thp2, connects transcription elongation with mitotic recombination in Saccharomyces cerevisiae. *EMBO J.*, **19**, 5824–5834.
56. Chavez,S. and Aguilera,A. (1997) The yeast HPR1 gene has a functional role in transcriptional elongation that uncovers a novel source of genome instability. *Genes Dev.*, **11**, 3459–3470.
57. Stoimenov,I., Schultz,N., Gottipati,P. and Helleday,T. (2011) Transcription inhibition by DRB potentiates recombinational repair of UV lesions in mammalian cells. *PLoS One*, **6**, e19492.